

Supporting Information

Juryne et al. 10.1073/pnas.0806015105

SI Methods

Animals and Embryo Manipulations. AB strain zebrafish were used as WT. Embryos from natural spawnings were cultured and staged as described (1, 2). To inhibit gene expression, \approx 1-nl solution containing MO was injected into the yolk of one-cell embryos. To measure the efficacy of MO treatment, RT-PCR was performed on RNA isolated from 24-hpf WT or MO-injected embryos. To measure touch-responsiveness, 10 WT and 10 *sepN* morphant 24–72 hpf embryos were transferred to dishes with 0.5-cm increment markers along the x and y axis, embryos were touched near the ear with forceps and scored as to whether or not they moved >0.5 cm. The behavior of the two groups was significantly different (Fisher's exact test). Gastrula stage transplants were performed as described (3): donor WT or MO-injected one-cell embryos were injected with Alexa Fluor 546 Dextran tracer dye, raised to the shield stage, 15–20 slow or fast fiber precursor cells were removed from the margin and transplanted homotopically to WT embryos of the same stage. Embryos were fixed at 24 hpf and processed for F59 (for slow fiber analysis) or F310 (for fast fiber analysis) antibody staining.

Morpholino Oligonucleotide Injections. Sequence for the SepN cDNA derived from the AB strain was deposited in GenBank (accession no. DQ160295). The following splice-blocking antisense MOs (Gene Tools) were used: *sepN* MO1 (E1D) 5'-GAATTGT-GAACTTACGTGTCGTTTC-3', *sepN* MO2 (E2D) 5'-GGGAT-AGTAATACCTGTGAGTTTT-3', *ryr1a* E2A 5'-CCTGGT-CATCCTACAAGAAAACGGT-3', *ryr1a* E3D 5'-TCTGTACAAACCTCATTAAGCTCAG-3', *ryr3* E1D 5'-GAGCGGCTTTTTACTTACAGTCCG-3'. To measure the efficacy of MO treatment, RT-PCR was performed on RNA isolated from 24-hpf WT or MO-injected embryos. Primers used for RT-PCR amplified the exon-intron boundaries targeted by the MOs. Primers used: SepN EIF 5'-GCATCAAATATTACCTGG-3', SepN E3R 5'-GTGGAATCTCCTCTTCAT-3', RyR1a E2F 5'-CCAGGTGGTGCTACAGTGTACAG-3', RyR1a E3R 5'-GTCAGTAGTGTAGCCAGCATC-3', RyR1a E3F 5'-GAT-GCTGGCTAACACTACTGAGC-3', RyR1a E6R 5'-GC-CAGTTTGTCTGTGAGGGATC-3', RyR3 E1F 5'-GCCGAAGGTGAAGGGGAAG-3', and RyR3 E2R 5'-CTTGGCCTCTGATGTGGGC-3'. Primers detecting *erm*, which encodes a transcription factor and whose expression is regulated by FGF signaling (5, 6), were used as a control: *erm* F 5'-GCAAGTCCCTTTCATGGTGC-3' and *erm* R 5'-GTGTTGC-CGTGCTGGAGG-3'.

In Situ Hybridization (ISH) and Immunohistochemistry (IHC). Whole-mount ISH was performed under standard conditions (1). The following ISH probes were used: *sepN*, *ryr1a*, and *ryr3* (see main text), *dystrophin* (7), *alpha cardiac actin* (D.J.G., unpublished data), *myoD* (8), *isl2* (9), *tal2* (10), and *c-ret* (11). For IHC with S58, embryos were fixed in Carnoy's solution overnight at 4°C (12). For all other antibodies, embryos were fixed with fresh 4% paraformaldehyde in PBS at room temperature for 4 h. Antibodies used for IHC were obtained from the Developmental Studies Hybridoma Bank and used at the following dilutions: F59 (1:5), F310 (1:3), S58 (1:5), *znpl* (1:5), 4D9 (1:5), and 34C (1:5). Anti-No Tail antibody (13) was used at 1:10,000 dilution.

TUNEL Staining and Cyclopamine Treatment. Cyclopamine (LC Laboratories) was dissolved in DMSO and diluted to 100 μ M in embryo medium (1). WT embryos were soaked in 100 μ M

cyclopamine or equivalent DMSO in embryo medium beginning at the high stage. WT, cyclopamine-treated, and *sepN* MO-injected embryos were fixed at the three-somite stage with 4% paraformaldehyde in PBS overnight at 4°C and processed for TUNEL staining (Roche In Situ Cell Death Detection Kit) and IHC with anti-No Tail antibody (13). Nuclei were counterstained with 1 μ M TO-PRO-3 (Molecular Probes). Images were obtained with a Leica DMRXE laser scanning confocal microscope.

Transmission Electron Microscopy. Twenty-four-hpf WT control and *sepN* morphant embryos were fixed overnight at 4°C in 2% glutaraldehyde and 2% paraformaldehyde in 0.1 M sodium cacodylate buffer, pH 7.2. Embryos were postfixed in 2% osmium tetroxide in 0.1 M sodium cacodylate for 45 min at room temperature, incubated in aqueous uranyl acetate for 45 min at room temperature, and dehydrated through an EtOH series. Embryos were embedded in epoxy resin, sectioned, and viewed by transmission electron microscopy.

RyR and SepN Cofractionation and Coimmunoprecipitation (co-IP). Soluble membrane fractions were prepared from rabbit back muscle as described (14). Equal quantities (20 μ g protein/lane) of each membrane subfraction were resolved by SDS/PAGE, transferred to nitrocellulose, and immunoblotted using anti-RyR-peptide antiserum (15) recognizing all RyR forms (α -pan-RyR, 1:2,000 dilution) or anti-SepN-MH4-peptide antiserum (α -SepN, 1:500 dilution) in the presence or absence of 10 μ g/ml MH4 peptide (CNKLVSILLWGA). For IP studies, rabbit skeletal muscle SR was prepared and solubilized as described (16), except DTT was omitted from all buffers. Solubilized SR protein was incubated with protein A-agarose and cleared by centrifugation at 100 g_{max} for 2 min. Supernatants were incubated with 1:200 anti-pan-RyR antiserum. Immune complexes were collected with protein A-agarose, solubilized in sample buffer containing 10 mM DTT and resolved on a 7.5% SDS/PAGE minigel and immunoblotted as above. Washed blots were incubated with 1:2,000 anti-rabbit IgG horseradish peroxidase conjugate and developed by using ECL Plus reagents. For the zebrafish co-IP experiments, sequences encoding the FLAG antigen were inserted in frame at the 3' end of the zebrafish *sepN* coding sequence, upstream from the natural *sepN* 3'UTR containing the SECIS element. The entire gene fusion was cloned into the CS2⁺ vector. mRNA was synthesized *in vitro* (Message Maker Kit, Epicentre Biotechnology) and injected into fertilized eggs. Approximately 250 14- to 18-somite-stage control or mRNA-injected embryos were solubilized (16), proteins were IP after incubation with anti-FLAG M2 affinity gel (Sigma), and recovered proteins were resolved by electrophoresis through 4–20% polyacrylamide gradient gels. Blots of the gels were probed with anti-FLAG M2, anti-RyR3 (17), or anti-RyR1 antibody, and signal was developed following incubation with ECL Plus (GE Healthcare).

Ryanodine-Binding Scatchard Analysis. Embryo and muscle homogenates were prepared in muscle buffer (MB: 250 mM KCl, 15 mM NaCl, 20 mM Hepes, pH 7.4, 100 μ M EGTA, supplemented with Complete EDTA-free Protease Inhibitor Mixture, Roche Applied Science). Equilibrium ryanodine binding to zebrafish embryo homogenates was measured in binding buffer (BB: 250 mM KCl, 15 mM NaCl, 20 mM Hepes, pH 7.1, 200 μ M CaCl₂, 109 μ M EGTA) containing 0.5 mg/ml homogenized protein with

0–200 nM ryanodine, 4 nM [³H]ryanodine, 0.1 mg/ml BSA, and 0.1% CHAPS. Samples were incubated 20 h at RT to achieve equilibrium binding and reactions were terminated (4). Equilibrium ryanodine binding to human muscle homogenates (0.05 mg/ml) was measured at 37°C for 3 h in BB containing 0–200 nM ryanodine with 4–8 nM [³H]ryanodine. Scatchard analysis was based on a one-site model. $1/K_d$ and B_{max} were estimated from the equation $B/F = (B_{max}-B)/K_d$. K_d and B_{max} were derived from the mean of six independent measurements performed on three different sets of zebrafish embryo samples and four independent measurements performed with human muscle samples.

Redox Titrations. Redox-sensitive ryanodine binding was slightly modified from (4). The initial binding rate of ryanodine to homogenates was calculated from a linear regression fit of four time-dependent measurements. Homogenates of WT or SepN-depleted embryos (0.5 mg/ml in 0.2 ml BB) were pretreated with GSH, and binding was initiated by the addition of 8 nM [³H]ryanodine and various concentrations of GSSG and GSH to achieve desired solution redox potentials as described (4). Binding reactions at RT were terminated after 30, 60, 90, and 120 min. Homogenates of human muscle (0.5 mg/ml) were incubated at 37°C in BB containing 8 nM [³H]ryanodine, and bound ryanodine was measured at 4, 8, 12, and 16 min. For the SepN protein add-back experiment, 8X His-tagged zebrafish SepN was syn-

thesized *in vitro* and SepN protein (0.2 μg/ml) was added to *SEPNI* mutant human muscle homogenates before binding studies. Experiments were repeated three times. In redox titrations, the initial rate of ryanodine binding was measured vs. the solution redox potential as previously described (4).

Synthesis of Zebrafish SepN. An 8X His sequence was inserted in frame at the 3' end of the zebrafish *sepN* coding sequence and the gene-fusion coding sequence plus *sepN* 3'UTR were cloned into the CS2⁺ vector. Full length 8X His-tagged zebrafish SepN was synthesized in a coupled rabbit reticulocyte lysate transcription and translation system with modifications described below to optimize selenocysteine insertion efficiency (18). Reactions contained 80% TnT Rabbit Reticulocyte Lysate, 1 mM methionine, 0.4 mM spermidine, 0.01 μg/ml SepN-8X-His DNA, and 300 nM of the C-terminal fragment of Secis Binding Protein 2 (SBP2) in a total of 800 μl. Control reactions were identical with the exception that no exogenous SBP2 was added. The addition of SBP2 is required for efficient incorporation of selenocysteine in RRL translation systems (18, 19). Reactions were incubated at 30°C for 2 h. The resulting His-tagged SepN was partially purified using a Ni²⁺ affinity MagZ Protein Purification System (Promega). The protein was concentrated using a Centricon 30 spin column (Millipore) and buffered in 250 mM KCl, 15 mM NaCl, 20 mM Hepes, pH 7.4, 100 μM EGTA.

1. Westerfield M (2000) *The Zebrafish Book* (Univ. of Oregon Press, Eugene).
2. Kimmel CB, Ballard WW, Kimmel SR, Ullmann B, Schilling TF (1995) Stages of embryonic development of the zebrafish. *Dev Dyn* 203:253–310.
3. Hirsinger E, Stellabotte F, Devoto SH, Westerfield M (2004) Hedgehog signaling is required for commitment but not initial induction of slow muscle precursors. *Dev Biol* 275:143–157.
4. Xia R, Stangler T, Abramson JJ (2000) Skeletal muscle ryanodine receptor is a redox sensor with a well defined redox potential that is sensitive to channel modulators. *J Biol Chem* 275:36556–36561.
5. Munchberg SR, Ober EA, Steinbeisser H (1999) Expression of the Ets transcription factors *erm* and *pea3* in early zebrafish development. *Mech Dev* 88:233–236.
6. Roehl H, Nusslein-Volhard C (2001) Zebrafish *pea3* and *erm* are general targets of FGF8 signaling. *Curr Biol* 11:503–507.
7. Bassett DL, et al. (2003) Dystrophin is required for the formation of stable muscle attachments in the zebrafish embryo. *Development* 130:5851–5860.
8. Weinberg ES, et al. (1996) Developmental regulation of zebrafish MyoD in wild-type, no tail and spadetail embryos. *Development* 122:271–280.
9. Appel B, et al. (1995) Motoneuron fate specification revealed by patterned LIM homeobox gene expression in embryonic zebrafish. *Development* 121:4117–4125.
10. Pinheiro P, Gering M, Patient R (2004) The basic helix-loop-helix transcription factor, Tal2, marks the lateral floor plate of the spinal cord in zebrafish. *Gene Expr Patterns* 4:85–92.
11. Bisgrove BW, Raible DW, Walter V, Eisen JS, Grunwald DJ (1997) Expression of *c-ret* in the zebrafish embryo: potential roles in motoneuronal development. *J Neurobiol* 33:749–768.
12. Devoto SH, Melancon E, Eisen JS, Westerfield M (1996) Identification of separate slow and fast muscle precursor cells *in vivo*, prior to somite formation. *Development* 122:3371–3380.
13. Schulte-Merker S, Ho RK, Herrmann BG, Nusslein-Volhard C (1992) The protein product of the zebrafish homologue of the mouse *T* gene is expressed in nuclei of the germ ring and the notochord of the early embryo. *Development* 116:1021–1032.
14. Saito A, Seiler S, Chu A, Fleischer S (1984) Preparation and morphology of sarcoplasmic reticulum terminal cisternae from rabbit skeletal muscle. *J Cell Biol* 99:875–885.
15. O'Driscoll S, et al. (1996) Calmodulin sensitivity of the sarcoplasmic reticulum ryanodine receptor from normal and malignant-hyperthermia-susceptible muscle. *Biochem J* 319:421–426.
16. Mackrill JJ, O'Driscoll S, Lai FA, McCarthy TV (2001) Analysis of type 1 ryanodine receptor-12 kDa FK506-binding protein interaction. *Biochem Biophys Res Commun* 285:52–57.
17. Giannini G, Conti A, Mammarella S, Scrobogna M, Sorrentino V (1995) The ryanodine receptor/calcium channel genes are widely and differentially expressed in murine brain and peripheral tissues. *J Cell Biol* 128:893–904.
18. Howard MT, Moyle MW, Aggarwal G, Carlson BA, Anderson CB (2007) A recoding element that stimulates decoding of UGA codons by Sec tRNA[Ser]Sec. *RNA* 13:912–920.
19. Copeland PR, Fletcher JE, Carlson BA, Hatfield DL, Driscoll DM (2000) A novel RNA binding protein, SBP2, is required for the translation of mammalian selenoprotein mRNAs. *EMBO J* 19:306–314.

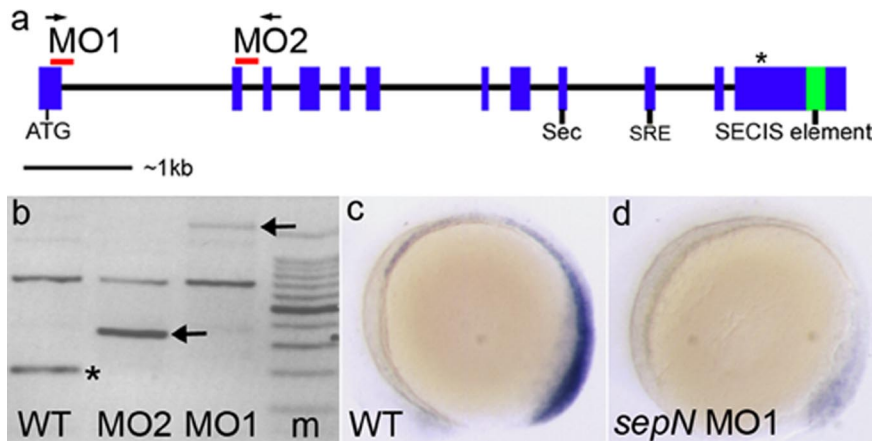


Fig. 51. SepN genomic structure and morpholino inhibition of SepN expression. (a) Genomic structure of the zebrafish *sepN* locus containing conserved elements including a selenocysteine codon (Sec), a Sec Redefinition Element (SRE), and a selenocysteine insertion sequence (SECIS) element. * indicates stop codon; red bars indicate sbMOs; arrows indicate primers used to detect *sepN* transcripts by RT-PCR. (b) RT-PCR analysis of *sepN* transcripts in 24 hpf WT, MO1- or MO2-injected embryos. *, WT *sepN* amplicon; arrows, intron-included amplicons; m, markers. (c and d) *sepN* RNA levels are reduced in MO1-injected embryos. Lateral views with rostral left.

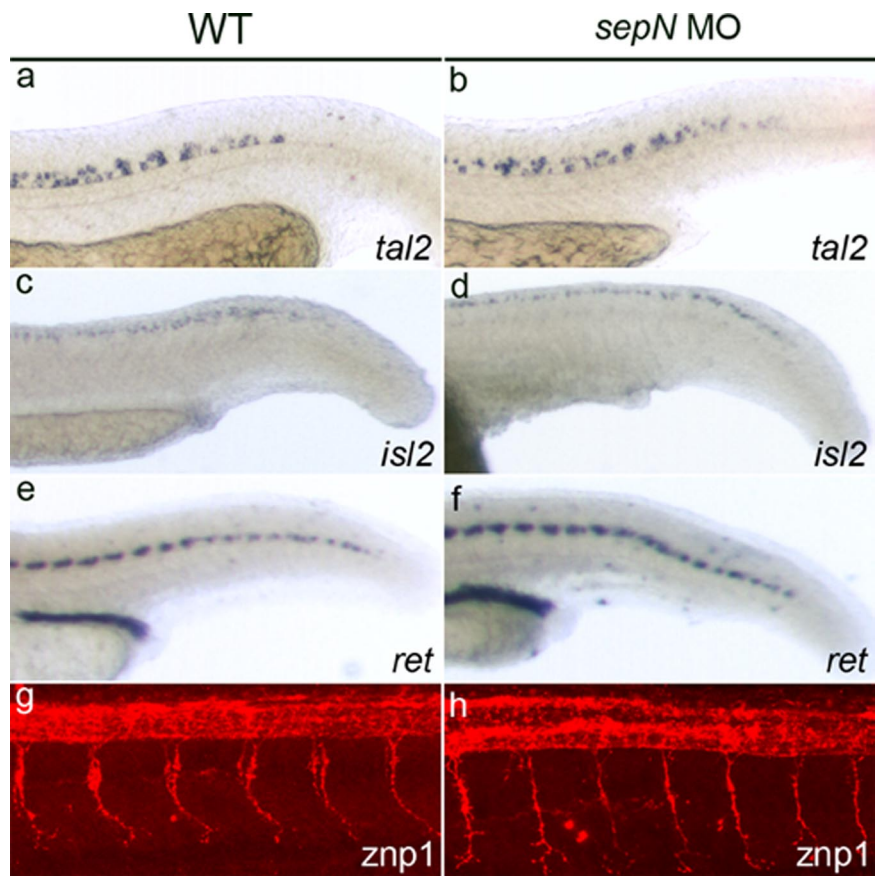


Fig. S2. Loss of SepN does not affect neural patterning or motor neuron projections. Expression of *tal2* (a and b), *isl2* (c and d), and *ret* (e and f) in 24 hpf WT and *sepN* morphants. Znp1 immunoreactivity in motor neurons in 24 hpf WT (g) and *sepN* (h) morphants.

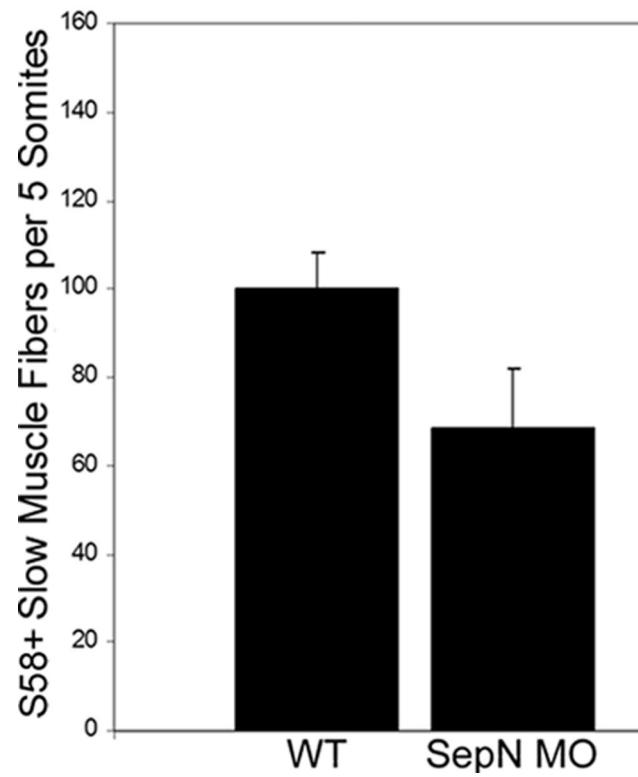


Fig. S3. Embryos lacking SepN have reduced numbers of slow muscle fibers. The numbers of S58⁺ fibers in the dorsal and ventral halves of 5 consecutive mid-trunk somites (over the yolk extension) were counted in 24 hpf embryos ($n = 25$ embryos for each group). *sepN* morphants exhibit a 32% reduction in the number of S58⁺ fibers as compared with WT controls. Asterisk indicates $P < 0.0005$ using Student's t-Test. Error bars are \pm SD.

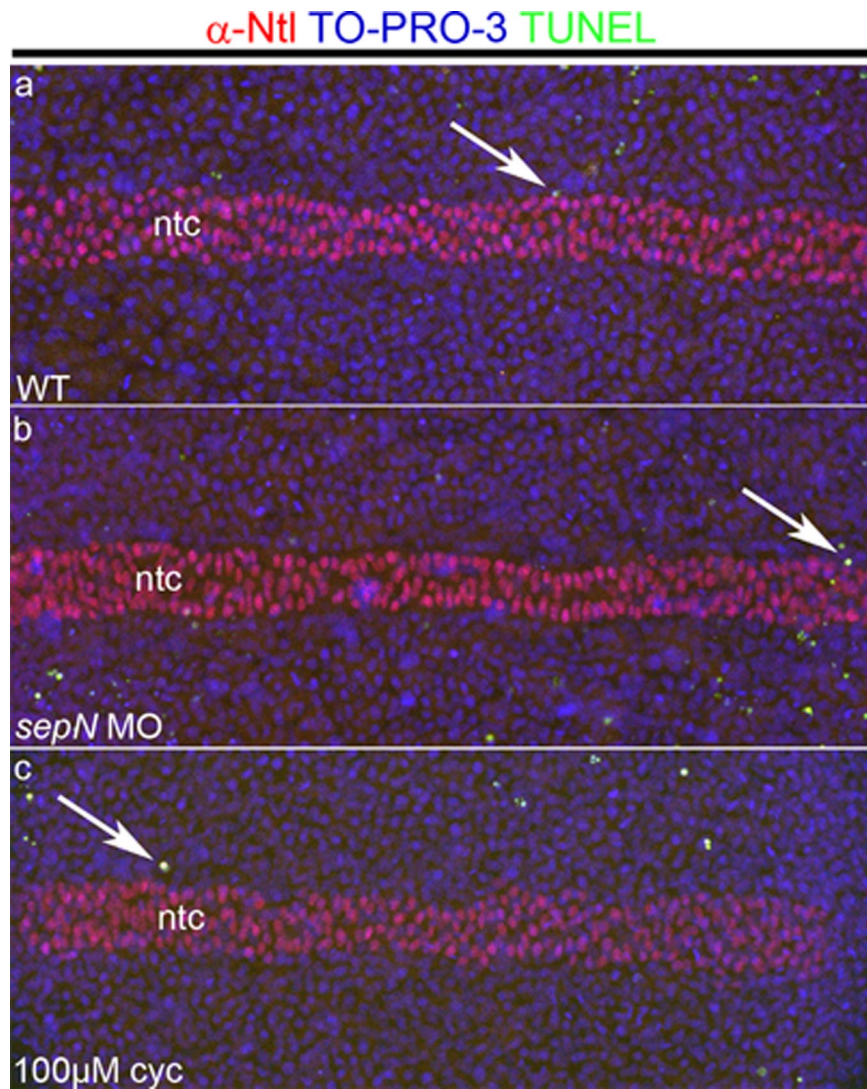


Fig. S4. Loss of SepN does not affect cell death among adaxial cells. Cell death was measured in somitic mesoderm of three-somite stage WT (a) or *sepN* morphant (b) embryos. As a control to detect cell death that might occur whenever adaxial cell differentiation was blocked, embryos treated with 100 μ M cyclopamine (c) were also examined. Adaxial cells form parallel rows of cells that lie immediately adjacent to the notochord and were visualized by a combination of staining for all nuclei (TO-PRO-3, blue) and for the No Tail protein, a marker of notochord (ntc) nuclei (α -Ntl, red). Apoptotic cells were visualized with TUNEL assay (green). Arrows indicate TUNEL-positive cells in the adaxial region, observed in similar numbers in control and treated embryos. Dorsal views with rostral left.

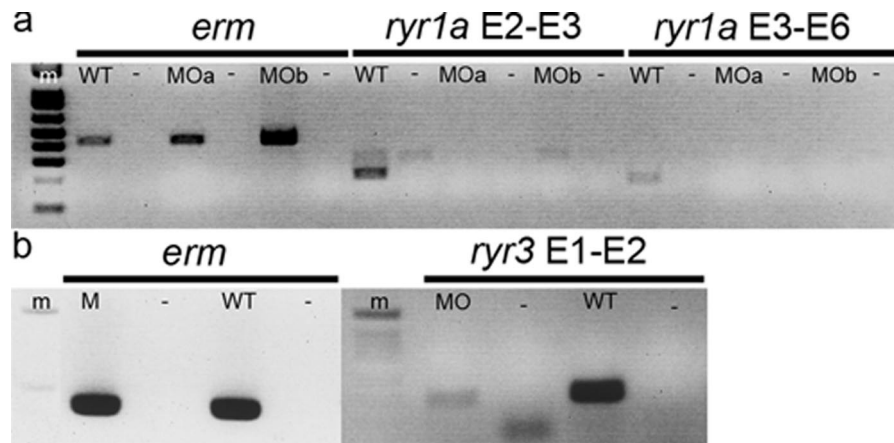


Fig. S5. Determination of transcript production in *ryr* morphant embryos. (a) Embryos were mock-injected (WT) or injected with a combination of two *ryr1a* sbMOs directed at the exon 2 splice acceptor and the exon 3 splice donor sites. RNA was analyzed from two independent injected groups, MOa and MOb. Transcripts were analyzed by RT-PCR at 24 hpf for production of mature *erm* or *ryr1a* RNA. Two pairs of exon-specific primers (E2-E3 and E3-E6) were used to detect different regions of the *ryr1a* transcripts. No WT *ryr1a* transcripts were detected in morphants. (b) Embryos were mock-injected (WT) or injected with a *ryr3* sbMO directed at the exon 1 splice donor site. Transcripts were analyzed by RT-PCR at 24 hpf for production of mature *erm* or *ryr3* RNA. A pair of exon-specific primers (E1-E2) was used to detect *ryr3* transcripts. Decreased levels of WT *ryr3* transcripts were detected in morphants. Minus sign indicates negative control reactions performed without cDNA synthesis.

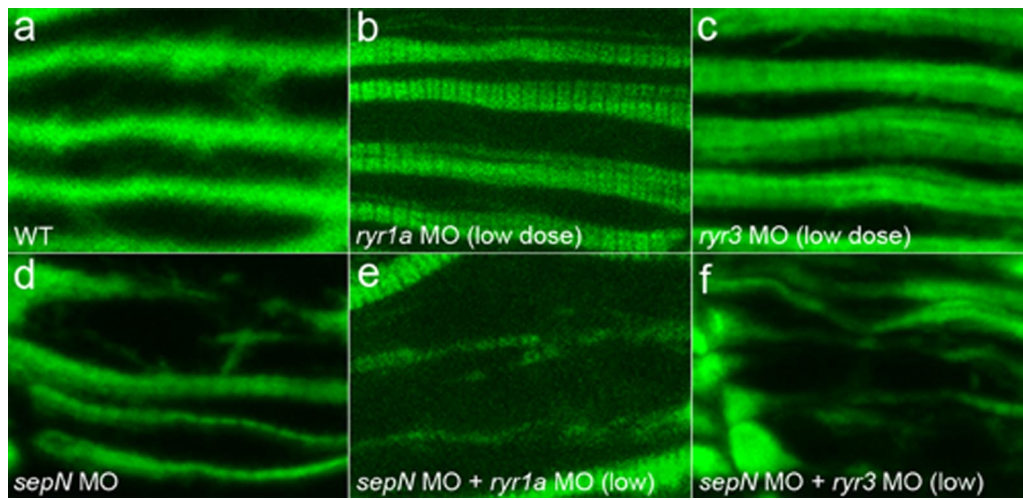


Fig. S6. SepN and RyRs have more than additive effects on slow fiber formation. (a-c) Mild reduction of RyR1a or RyR3 levels with low doses of MO has no detectable effect on morphology of F59⁺ slow muscle fibers. (d-f) Mild reduction of RyR1a or RyR3 in embryos depleted of SepN leads to significant enhancement of the disrupted slow muscle fiber phenotype. Lateral views, rostral left.

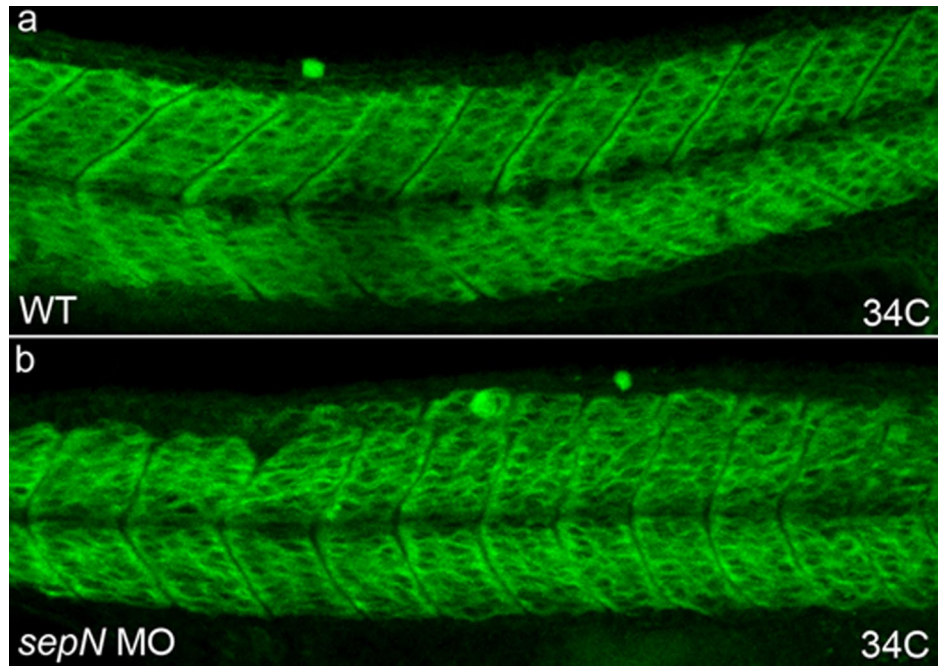


Fig. S7. *SepN*-depleted and WT control embryos have similar expression of RyR proteins. WT (a) and *SepN* MO-injected (b) embryos were analyzed for expression of RyR proteins by IHC with the 34C antibody. Lateral views, rostral left.

Table S1. Quantification of slow muscle phenotype in embryos with reduced SepN and RyR function

<i>sepN</i> MO and <i>ryr1a</i> MO coinjections				
MO injected	WT/mild	Moderate	Severe	Total embryos analyzed
WT Controls	27	0	0	27
<i>ryr1a</i> E3D 8 ng	34	4	0	38
<i>sepN</i> 4 ng	4	20	0	24
<i>ryr1a</i> E3D 8 ng + <i>sepN</i> 4 ng	1	14	22	37
<i>sepN</i> MO and <i>ryr3</i> MO coinjections				
WT Controls	44	0	0	44
<i>ryr3</i> E1D 1 ng	3	12	0	15
<i>sepN</i> 4 ng	7	24	1	32
<i>ryr3</i> E1D 1 ng + <i>sepN</i> 4 ng	0	7	20	27

Embryos were mock-injected or injected with MOs: 4 ng *sepN* MO (complete knockdown), 8 ng *ryr1a* E3D MO (mild knockdown), 1 ng *ryr3* E1D MO (mild knockdown), or combinations of *ryr1a* MO + *sepN* MO or *ryr3* MO + *sepN* MO. F59⁺ slow muscle cells were analyzed in 24 hpf embryos for degree of dysmorphology, fiber thickness, and fraction of affected fibers. Tabulation of fiber phenotype indicates a shift to a more severe phenotype when a low dose of *ryr* MOs is co-injected with *sepN* MOs. Embryos were scored blindly with respect to injection.